

YERIN KIM<sup>1</sup>, JI HYEON LEE<sup>2</sup>, JEA HYUNG KIM<sup>1</sup>, HYUN SEON HONG<sup>1\*</sup>

## EFFECTS OF DRY AND WET BALL MILLING ON THE STRUCTURAL AND OPTICAL PROPERTIES OF ZnO POWDER

Zinc oxide is a promising material for optoelectronic and UV-protection applications due to its biocompatibility, wide band-gap, and excellent optical properties. Since these properties are highly dependent on the microstructure, precise process control is essential for optimization. However, research on the high-value-added applications for ZnO recovered from industrial byproducts remains limited. In this study, the particle size and morphology of ZnO powder synthesized from waste zinc dust were controlled via dry and wet ball milling processes. The correlation between microstructural changes – driven by milling conditions such as rotational speed and process method – and the resulting optical properties, including UV transmittance and photoluminescence, was systematically investigated. The results showed that the microstructure and UV transmittance of the ZnO powders changed distinctly depending on the milling parameters. Notably, the wet ball milling condition at 600 rpm achieved a minimum transmittance of 10.0%, demonstrating superior UV-shielding performance. This study demonstrates that the structural and optical properties of waste-derived ZnO powder can be effectively tuned through the ball milling, suggesting the potential for utilizing industrial byproducts as functional UV-shielding materials.

*Keywords:* Zinc oxide; waste-derived materials; Ball milling; UV-shielding properties

### 1. Introduction

Zinc oxide (ZnO) has been extensively studied for various optoelectronic applications due to its low toxicity, excellent biocompatibility, wide bandgap, and superior optical properties [1-2]. ZnO possesses a relatively high refractive index and strong light-scattering characteristics, which are highly dependent on microstructural factors such as particle size, morphology, crystallinity, and state of aggregation [3]. Therefore, precise process design to control the microstructure is essential for tuning the optical properties of ZnO powders.

Various studies have been tried to manipulate the microstructure of ZnO by adjusting particle sizes from the nano- to micrometer scale or by altering particle shapes. Among these methods, mechanical grinding is advantageous because it is relatively simple, scalable, and capable of simultaneously inducing particle size reduction and morphological changes [4-6]. However, the particle fragmentation mechanism and the resulting structural transformations can vary significantly depending on the grind-

ing method and processing conditions. In particular, dry and wet ball-milling processes result in distinct microstructures due to their differing collision and shear behaviors.

Meanwhile, most commercially available ZnO powders are currently manufactured from refined primary raw materials, and research on recycling industrial byproducts containing zinc remains relatively scarce [7-8]. In terms of resource circulation and sustainability, developing processes to convert waste zinc into functional ZnO is recognized as a critical research challenge. Nevertheless, studies linking microstructural control with the optical properties of waste-zinc-derived ZnO have not yet been sufficiently conducted.

In this study, ZnO powder synthesized from waste zinc dust was subjected to dry and wet ball-milling processes to control its particle size and morphology. By establishing the correlation between the structural control of waste-zinc-based ZnO powder and its optical properties, such as UV transmittance, this research demonstrates the potential for high-value utilization of industrial byproducts.

<sup>1</sup> SUNGSHIN WOMEN'S UNIVERSITY, DEPARTMENT OF MATERIALS SCIENCE AND ENGINEERING SEOUL, 01133, REPUBLIC OF KOREA

<sup>2</sup> GRADUATE SCHOOL, SUNGSHIN WOMEN'S UNIVERSITY, DEPARTMENT OF NEXT-GENERATION APPLIED SCIENCE, SEOUL, 01133, REPUBLIC OF KOREA

\* Corresponding author: [hshong@sungshin.ac.kr](mailto:hshong@sungshin.ac.kr)



## 2. Experimental

### 2.1. Materials

The zinc oxide (ZnO, 99.48%) powder used in this study has a median particle size (D50) of 10.9  $\mu\text{m}$  and exhibits a rod morphology. The high-purity samples were provided by Korea Institute of Geoscience and Mineral Resources (KIGAM) for use in the experiments. For the wet ball-milling process, ethanol (EtOH,  $\geq 99.9\%$ , Duksan Pure Chemicals) was employed as the solvent.

### 2.2. Ball-Milling of ZnO Powder

Ball milling was performed under both dry and wet conditions using a planetary ball mill (FRITSCH). A 45-mL zirconia jar and zirconia grinding balls with a diameter of 3 mm were utilized for the milling process. For dry ball milling, the ball-to-powder mass ratio (BPR) was fixed at 20:1. The rotational speeds were set to 200, 400, and 600 rpm. For each condition, the ball milling process was conducted for 4 hours, after which the resulting powder was collected. For wet ball-milling process, the BPR was also maintained at 20:1, with ethanol (EtOH) used as the solvent. The rotational speeds and milling time were kept identical to the dry conditions at 200, 400, and 600 rpm for 4 hours. Following the milling process, the samples were dried at 70°C for 5 hours to remove the residual solvent before the final powder was recovered.

### 2.3. Characterization

The morphology of the ZnO powders was analyzed using field-emission scanning electron microscopy combined with energy-dispersive X-ray spectroscopy (FE-SEM/EDS; JSM-7500F, JEOL, Japan). The crystal structure of the powders was characterized by X-ray diffraction (XRD; D8 Focus, Bruker, Germany). The particle size distribution was measured using a particle size

analyzer (PSA; Nano Plus HD, Micromeritics, USA). The photoluminescence (PL) properties of the ZnO powders were analyzed using a PL spectrometer (FP-8500, Jasco, Japan), and the optical transmittance characteristics were evaluated using a UV-Vis spectrometer (SPECORD PLUS, Analytik Jena, Germany).

## 3. Results and discussion

Fig. 1 shows the SEM images of the raw ZnO powder and the ZnO powders ball-milled at various rotational speeds under both dry and wet conditions. Under wet conditions (b-c), the smooth rod-like morphology of the raw material was relatively well maintained at 200 rpm, but as the rpm increased, the particles fractured into irregular fragments and became finer. In contrast, under dry conditions (d-f), the particles tended to fracture into more rounded shapes with increasing rpm. This difference is attributed to the dominance of direct mechanical collisions in dry conditions, which induce not only particle fracture but also surface abrasion and re-agglomeration, leading to rounded morphologies. In wet conditions, although the liquid medium acts as a buffer that partially reduces direct impact-induced surface abrasion, it simultaneously suppresses particle re-agglomeration. As a result, particle fragmentation proceeds more effectively under wet conditions within the same rotational speed range, leading to a finer and more uniform particle size distribution. In particular, under dry conditions, no significant further morphological change was observed at 600 rpm compared to 400 rpm, whereas continuous refinement was evident under wet conditions.

The XRD results in Fig. 2 reveal distinct diffraction peaks at 2theta values of 31.9° (100), 34.6° (002), and 36.5° (101) for all samples, corresponding to the hexagonal wurtzite ZnO single phase [9]. No diffraction peaks from secondary phases were observed after ball milling. As the rpm increased, the full width at half maximum (FWHM) of the XRD peaks increased, indicating crystallite size reduction and decreased crystallinity [10]. For instance, the FWHM of the (101) peak increased from 0.13° before ball milling to 0.62° and 0.54° at 600 rpm, corresponding to approximately 4.7 and 4.2 times higher values under wet and

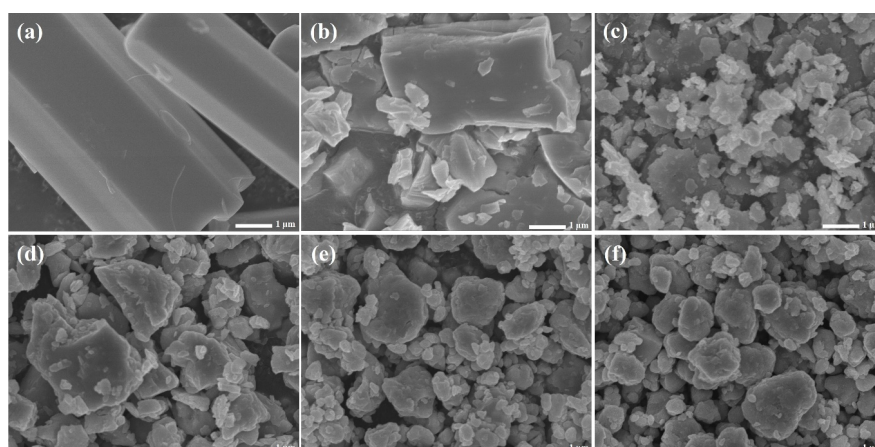


Fig. 1. SEM images of (a) raw ZnO powder and ball-milled ZnO powders under various conditions: wet-milled at (b) 200 rpm, (c) 600 rpm; and dry-milled at (d) 200 rpm, (e) 400 rpm, and (f) 600 rpm

dry conditions, respectively. This is interpreted as a result of the reduction in crystallite size caused by repeated mechanical deformation during the milling process, which leads to the observed degradation in the crystallinity of the ZnO powder [2,6,10,11].

The particle size distribution results (TABLE 1) also confirm that the distribution shifted toward smaller particle regions with increasing rpm for both dry and wet samples. The wet-milled samples formed a relatively uniform and finer particle size distribution. This suggests that non-uniform fracturing and agglomeration occur simultaneously under dry conditions, whereas the liquid medium induces more uniform refinement under wet conditions. Consequently, these PSA results indicate that wet ball-milling is more effective in achieving substantial particle refinement, which supports the microstructural observations from the SEM analysis.

TABLE 1

Particle size distribution parameters (mean diameter, D10, D50, and D90) of ZnO powders ball-milled under dry and wet conditions at various rotational speeds

Mode	rpm	Mean. (nm)	D10 (nm)	D50 (nm)	D90 (nm)
Dry	200	1176	804	1091	1509
	400	905	650	847	1116
	600	860	384	724	1417
Wet	200	1256	888	1173	1573
	400	711	467	661	943
	600	626	305	541	1000

The structural dependence of the optical properties of the ball-milled ZnO powders was investigated using PL measurements. Figs. 3(a) and 3(b) present the PL spectra of the ZnO

powders after dry and wet ball milling, respectively. Compared to the raw ZnO (indicated by the dashed lines), the emission intensity in the visible region significantly decreased following the ball milling process, which is consistent with previous findings reported in the literature [10]. Visible emission in the PL spectra of ZnO is widely reported as defect-level emission originating from crystal defects such as oxygen vacancies ( $V_O$ ) and zinc interstitials (Zni) [11,12]. In this study, the reduction rate of emission intensity at a wavelength of 514 nm was compared (Fig. 3(c)). A decrease in emission intensity was observed in all ball-milled samples. Notably, the reduction rate was most pronounced under dry milling conditions and high rpm, where direct mechanical impact and increased collision energy effectively suppressed the defect-related luminescent centers.

Fig. 4 shows the UV-Vis transmittance spectra of the ZnO powders after ball-milling compared to the raw ZnO. While the raw ZnO exhibited a high transmittance of over 94%, a significant reduction in transmittance was observed under all milling conditions [13]. However, the transmittance behavior did not exhibit a simple linear correlation with the rotational speed or the milling method. In the dry process, a minimum transmittance of 29.3% was observed at 400 rpm, while the wet process reached its lowest transmittance of 10.0% at 600 rpm. Based on the fundamental relationship between absorbance ( $A$ ) and transmittance ( $T$ ), defined as Eq. (1), these low transmittance values signify that the corresponding samples possess significantly higher optical density and shielding capabilities against incident light [14-15].

$$A = -\log_{10}(T) \quad (1)$$

While a relatively uniform transmittance was maintained within the 300-700 nm range under dry and low-speed wet con-

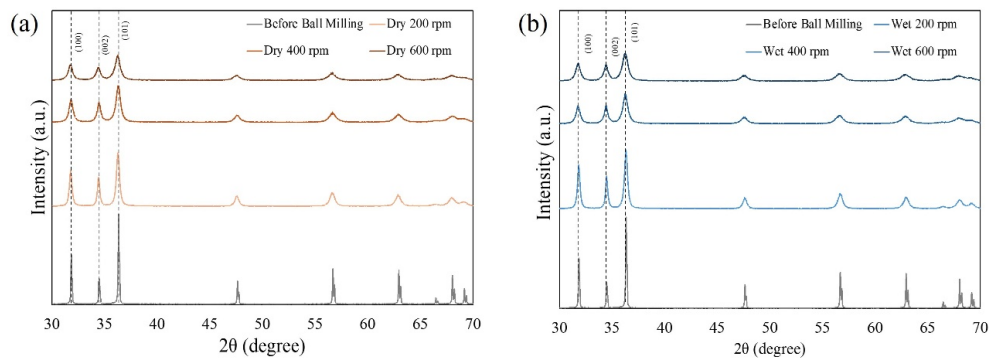


Fig. 2. XRD patterns of raw ZnO and ball-milled ZnO powders at different rotational speeds: (a) dry-milling conditions and (b) wet-milling conditions

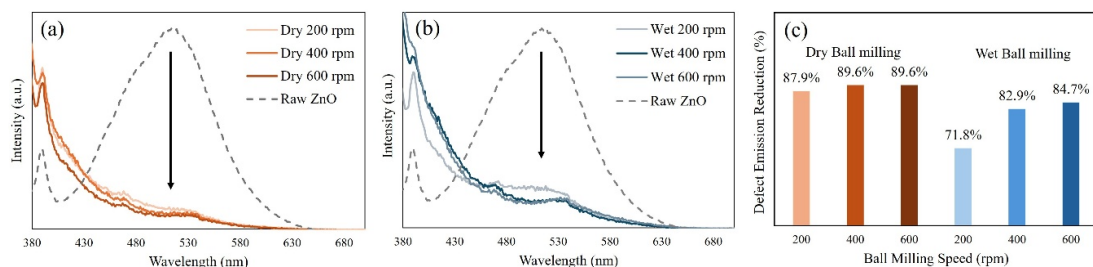


Fig. 3. PL spectra of ZnO powders milled under (a) dry and (b) wet conditions at various rotational speeds, and (c) the reduction rate of the defect-related emission intensity at 514 nm

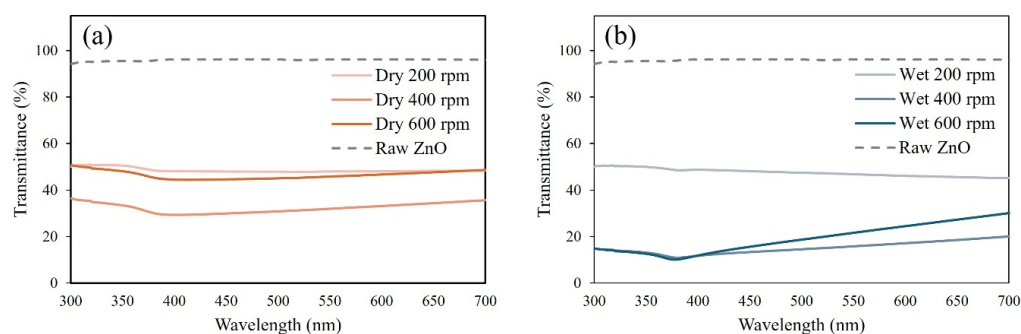


Fig. 4. UV-Vis transmittance spectra of ZnO powders ball-milled under (a) dry and (b) wet conditions

ditions, the 600 rpm wet-milled sample exhibited a pronounced decrease in transmittance in the UV region (300-380 nm), followed by a sharp increase beyond ~378 nm, a typical absorption behavior of semiconductors [16-18]. This enhanced performance at 600 rpm under wet conditions is attributed to the formation of a finer and more uniform particle structure, resulting from suppressed re-agglomeration and more effective fragmentation, which leads to enhanced UV attenuation [19].

#### 4. Conclusion

In this study, the structural and optical characteristics of ZnO powders were investigated under various ball-milling conditions. The results demonstrated that the particle morphology, defect-related photoluminescence, and UV transmittance properties varied distinctly depending on the milling method and rotational speed; in particular, the high speed wet ball milling condition exhibited superior UV-shielding performance. These findings suggest that the optical properties of ZnO powders can be selectively controlled and optimized through the ball-milling process. Ultimately, by establishing a clear correlation between the structural modification of waste-derived ZnO powders and their optical functionalities, such as UV transmittance, this research highlights a viable pathway for transforming industrial byproducts into high-value-added functional materials.

#### Acknowledgments

This work was supported by the Technology Innovation Program (RS-2024-0044834, Development of 4N grade zinc oxide production technology using carbon-reducing pyro-metallurgy from zinc dust) funded By the Ministry of Trade Industry & Energy (MOTIE, Korea)

#### REFERENCES

- [1] S. Wirunchit, P. Gansa, W. Koetniyom, *Materials Today: Proceedings* **47**, 3554-3559 (2021).
- [2] L.C. Damonte, L.A. Mendoza Zélis, B. Marí Soucase, M.A. Hernández Fenollosa, *Powder Technology* **148**, 15-19 (2004).
- [3] A. Kołodziejczak-Radzimska, T. Jesionowski, *Materials* **7**, 2833-2881 (2014).
- [4] Salah, Numan, Sami S. Habib, Zishan H Khan, Adnan Memic, Ameer Azam, Esam Alarfaj, Nabeel Zahed, Salim Al-Hamed, *International Journal of Nanomedicine* **6**, 863-869 (2011).
- [5] Jasvir Singh, Shivani Sharma, Sumedha Soni, Sandeep Sharma, Ravi Chand Singh, *Materials Science in Semiconductor Processing* **98**, 29-38 (2019).
- [6] Sajjad Amir Khanlou, Mostafa Ketabchi, Nader Parvin, *Materials Letters* **86**, 122-124 (2012).
- [7] <https://www.vizorsun.com/manufacturers-of-zinc-oxide-how-they-differ-and-why-the-process-matters/>
- [8] Amir Moezzi, Andrew M. McDonagh, Michael B. Cortie, *Chemical Engineering Journal* **185-186**, 1-22 (2012).
- [9] Ananthu C. Mohan, B. Renjanadevi, *Procedia Technology* **24**, 761-766 (2016).
- [10] W. Mekprasart, B.R. Ravuri, R. Yimnirun, W. Pecharapa, *ScienceAsia* **46**, 91-96 (2020).
- [11] M. Soosen Samuel, L. Bose, K. C. George, *Academic Review* **16**, 57-65. (2009).
- [12] Jinpeng Lv, Chundong Li, Ziyi Chai, *Journal of Luminescence* **208**, 225-237 (2019).
- [13] P. K. Giri, et al., *Journal of Applied Physics* **102**, 093515 (2007).
- [14] M. Sumukha, N. Shoshankumar, Saideep Shirish Bhat, S.C. Gurumurthy, V.K. Ashith, Neelamma B. Gummagol, Vighneshwar S. Bhat, Sanjeev R. Inamdar, V. Veena Devi Shastrimath, M.P. Shilpa, *Materials Science in Semiconductor Processing* **203**, 110227 (2026).
- [15] Jing Ge, Dingbo Han, Shuzhen Li, Jia Li, Song Hong, Ce Wang, Ping Hu, Seeram Ramakrishna, Yong Liu, *Separation and Purification Technology* **344**, 127310 (2024).
- [16] Khateeba Irshad, Muhammad Tahir Khan, Adil Murtaza, *Physica B: Condensed Matter* **543**, 1-6 (2018).
- [17] M. Milanese, G. Colangelo, A. Creti, M. Lomascolo, F. Iacobazzi, A. de Risi, *Solar Energy Materials and Solar Cells* **147**, 315-320 (2016).
- [18] Jing Shao, Honglie Shen, Kai Gao, Xiaomin Huo, Jaffer Siddique, Xuewen Wang, Weili Meng, *Optical Materials* **118**, 111287 (2021).
- [19] S.S. Alias, A.B. Ismail, A.A. Mohamad, *Journal of Alloys and Compounds* **499**, 231-237 (2010).